ADVANCED OPTICAL MATERIALS

Supporting Information

for *Adv. Optical Mater.*, DOI 10.1002/adom.202300135

Silicon Microspheres for Super-Planckian Light Sources in the Mid Infrared

Roberto Fenollosa, Fernando Ramiro-Manzano, Moises Garín and Francisco Meseguer*

WILEY-VCH

Supporting Information

Silicon Microspheres for Super-Planckian Light Sources in the Mid Infrared

Roberto Fenollosa, Fernando Ramiro-Manzano, Moises Garín and Francisco Meseguer*

R. Fenollosa, F. Ramiro-Manzano, F. Meseguer
Instituto Universitario de Tecnología Química, CSIC-UPV, Universitat Politècnica de València, Av. dels Tarongers, València 46022, Spain

E-mail: rfenollo@ter.upv.es

Moises Garín
GR-MECAMAT, Universitat de Vic – Universitat Central de Catalunya (UVIC-UCC), Campus Torre dels Frares, c/ de la Laura 13, 08500 Vic, Spain

Contents

S1. Obtained interferograms and system sensitivity correction.

S2. Approaches for the fitting process.

S3. Mie modes identification and field distributions.

S4. Thermal emission spectra of other silicon microspheres.

S5. Lorentizan fits to resonance peaks of M2.

S1. Obtained interferograms and system sensitivity correction.

Figures S1 and S3 show the as-recorded interferograms for M1(ϕ = 2080 nm, T = 660 ºC) and M2 (ϕ = 3730 nm, T = 560 ºC) respectively, and figures S2 and S4 show their corresponding spectra obtained after applying gaussian apodization to the interferograms and Fourier transform. The experimental emission spectra shown in figure 3 of the main text were achieved by correcting these spectra by the sensitivity curve of the system shown in figure S5. This correction curve was calculated by dividing the measured thermal emission spectrum of a bulk carbon body at 300 ºC (that we assumed to be quite approximate to a black body) by the theoretical spectrum of a black body at that temperature.

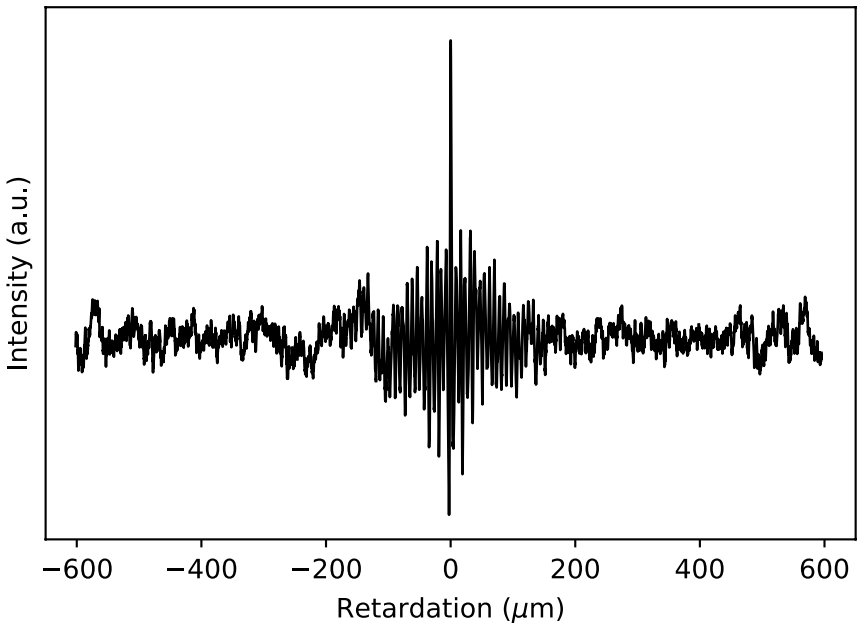

Figure S1. Interferogram corresponding to M1 (ϕ = 2080 nm, T = 660 ºC).

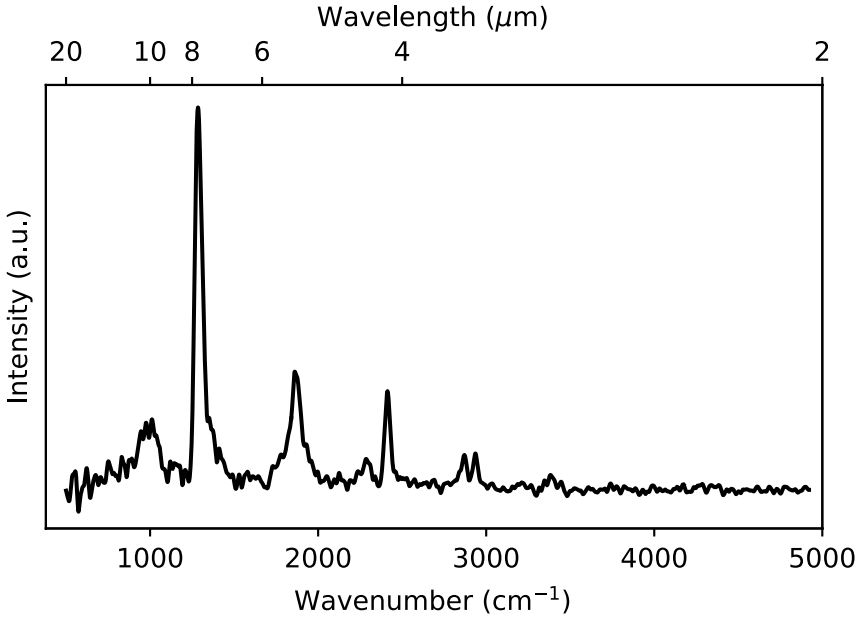

Figure S2. Thermal emission spectrum of M1 (ϕ = 2080 nm, T = 660 ºC) as obtained from the Fourier transform of the interferogram of Figure S1 after performing Gaussian apodization.[1] The spectrum is not corrected by the sensitivity of the system.

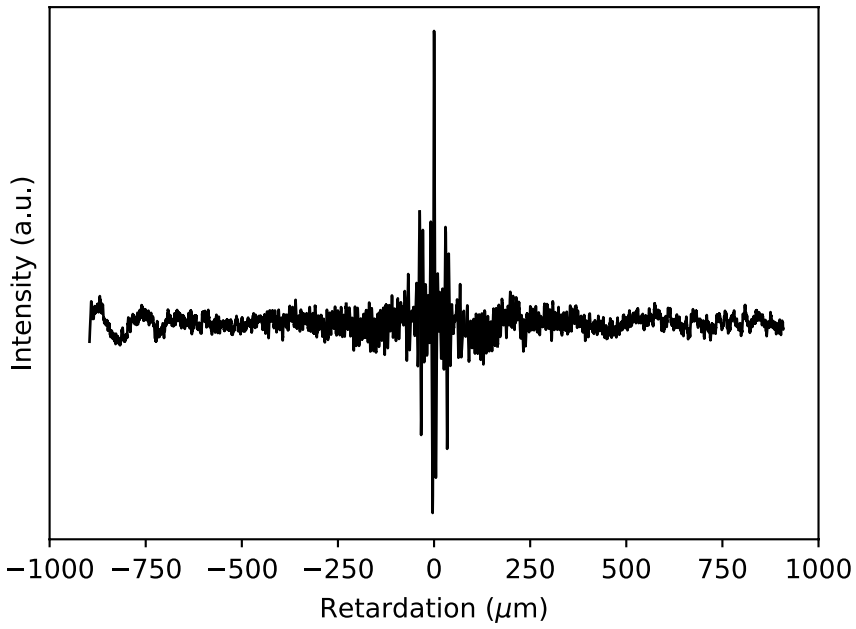

Figure S3. Interferogram corresponding to M2 (ϕ = 3730 nm, T = 560 ºC).

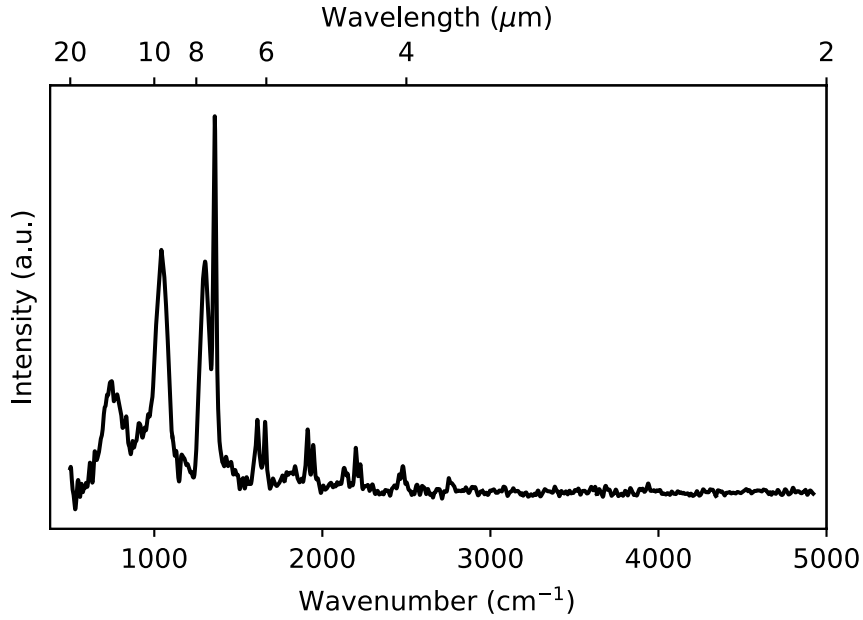

Figure S4. Thermal emission spectrum of M2 (ϕ = 3730 nm, T = 560 ºC) as obtained from the Fourier transform of the interferogram of Figure S3 after performing Gaussian apodization.[1] The spectrum is not corrected by the sensitivity of the system.

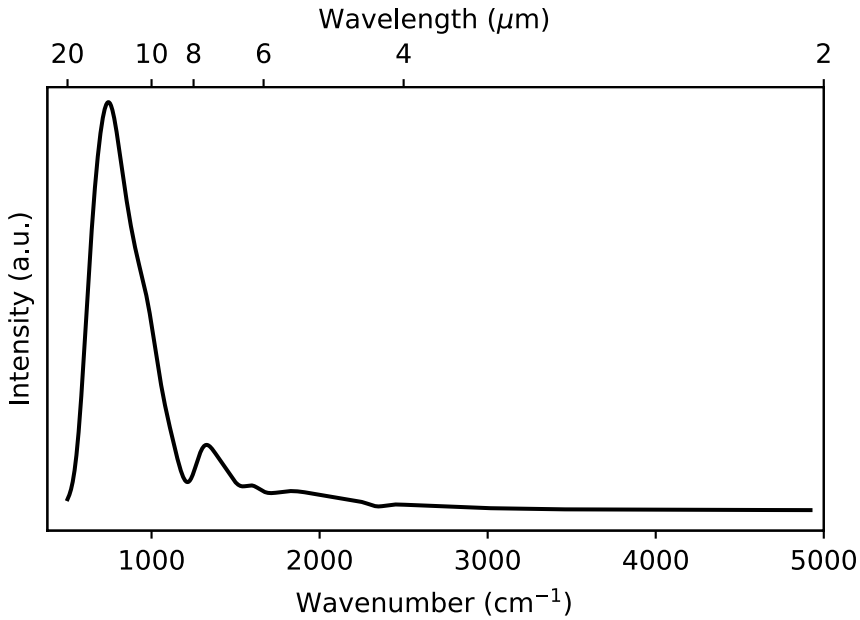

Figure S5. Sensitivity curve of the measuring set up. It was obtained by dividing the measured thermal emission spectrum of a bulk carbon body at 300 ºC by the theoretical spectrum of a black body at that temperature.

S2. Approaches for the fitting process.

We have assumed several approaches in the calculations that should be outlined. Firstly, as mentioned in the main text, although the emission corresponding to the lattice vibration of silicon appears in the wavelength range from 6 to 25 μm, this contribution has been disregarded because it is much lower than that originated from *FC* at the working temperatures of the experiments.[2] Secondly, based on previous experiments[3] we have considered here arbitrarily a fixed value of $1x10^{17}$ cm^{-3} for the density of *FC* associated to the blue laser, rather than a fit parameter. The reason is that this density influences mainly the relative height of the peaks, and there are unavoidable errors arisen from the sensitivity correction process that may deviate the height and width of some resonant peaks from their true values. This is the case, for instance of resonance $b_{1,1}$ of M1 [figure 3 (a)] whose experimental width and height are strongly influenced by the dip in the sensitivity correction curve (Figure S5) around 1200 cm^{-1}. All in all, the density of *FC* associated to the laser is lower than that originated from the temperature [$2x10^{17}$ cm^{-3} for the lower fitted temperature (560 ºC) corresponding to M2 in figure 3 (b)]. Thirdly, finite element simulations showed that the temperature is not uniform in all the sphere volume because the point where the microsphere contacts the supporting substrate works as a heat sink by conduction producing a vertical gradient of about 10 ºC.[3] Because the field image iris was totally opened during the experiments, we expect that all temperatures within this gradient contribute to the resonances. This is however in good agreement with the fitted temperature uncertainties (see Table 1 of main text).

S3. Mie modes identification and field distribution.

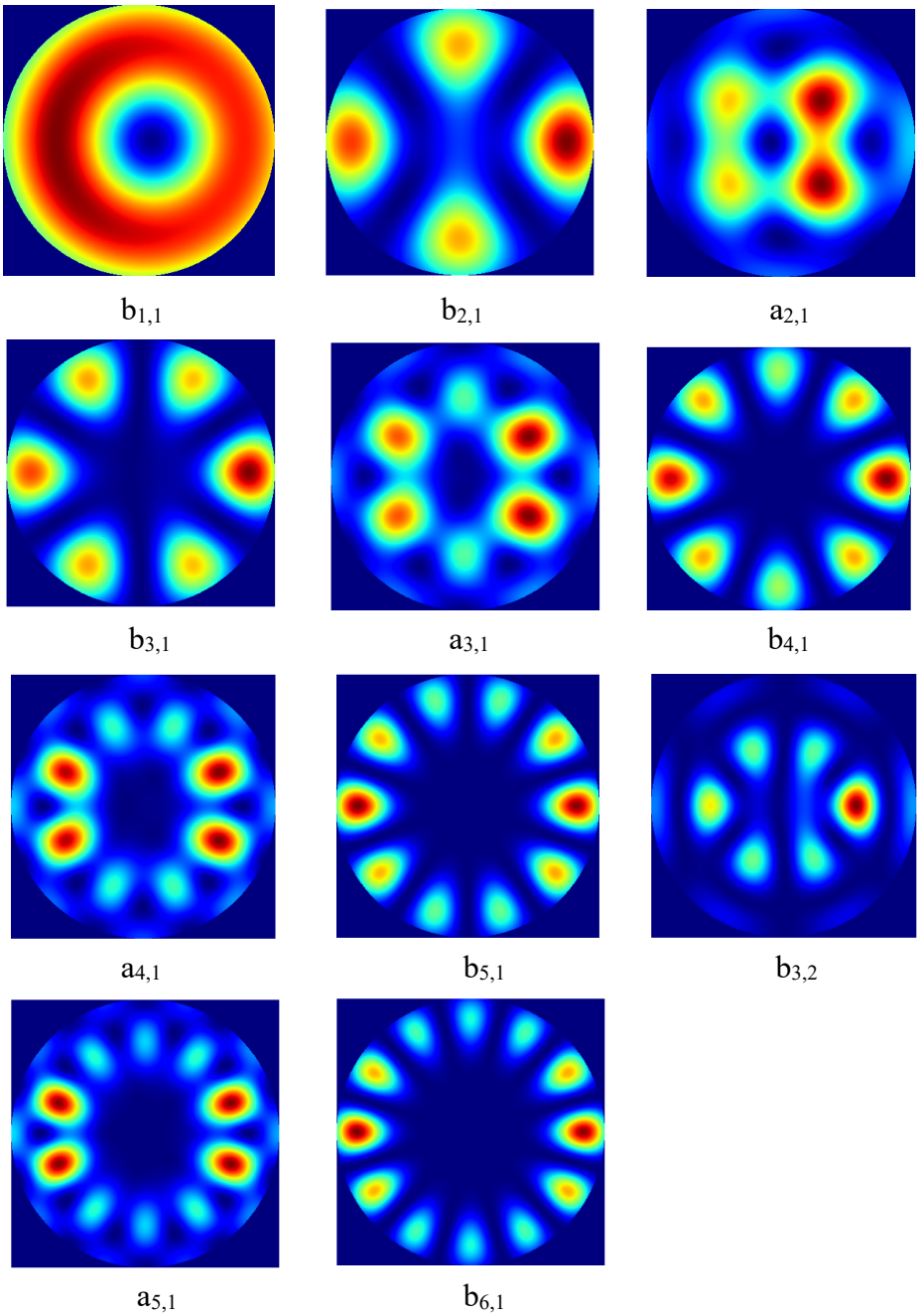

Figure S6. Internal electric field intensity distributions in the resonant plane of the modes involved in the thermal emission of silicon microspheres M1 and M2 of figure 3.

According to Mie theory, an electromagnetic field submitted to scattering and absorption processes by a sphere can be developed into a series of terms based on spherical harmonics and some coefficients, named as a_n and b_n where n=1,2,3…, that depend on the wavelength (λ), the refractive index contrast between the sphere and the surrounding

environment, and the sphere diameter (Φ).[4] The absorption efficiency [which equals the emissivity in eq. (1) of the main text] can be calculated in terms of such coefficients.

In order to account for the resonant peaks it is convenient to calculate the mentioned coefficients and the spectra as a function of the size parameter ($sp = \pi \Phi/\lambda$). Each coefficient has several maxima which gives rise to a family of resonant peaks. Then a second number 'm' is required for identifying the resonances of such family, with m=1 corresponding to that maximum that appears at the lowest size parameter. In summary, resonant Mie modes can be named as $a_{n,m}$ and $b_{n,m}$.[4,5] Because of their electromagnetic field distribution, they have a Transverse Magnetic or a Transverse Electric character respectively. In addition, the first index 'n' called as the mode number indicates the number of electric field intensity maxima in the half sphere perimeter, and the second index 'm' called as the order number accounts for the number of maxima in the radial direction. Figure S6 shows the internal electric field intensity distribution in the resonant plane of the modes responsible of the peaked intensities of figure 3 of the main text.

In order to associate each peak with its corresponding Mie resonance calculations of the emission spectra where the absorption efficiency includes a single multipolar term of the Mie series, *i. e.* a single a_n or b_n coefficient, were performed. Figure S7 (a), (b), (c) and (d) shows the experimental (black curve) of M1 and the theoretical fitted spectra considering all the multipoles of the Mie series (red curve) as well as the theoretical spectra with considering single multipolar b_n (blue curve) and a_n (green curve) terms: b_1, a_1; b_2, a_2; b_3, a_3; b_4, a_4 respectively. Because the first theoretical peak (starting from size parameter = 0) appears at a size parameter around 0.8 [figure S7 (a)] we deduce that it corresponds to resonance $b_{1,1}$. The coefficient b_1 yields a second maximum at a size parameter near 1.7, that we associated to resonance $b_{1,2}$. However this second maximum is very weak and could not be detected experimentally, therefore we didn't consider it in figure 3 (a). A similar case is that of resonance $a_{1,1}$.

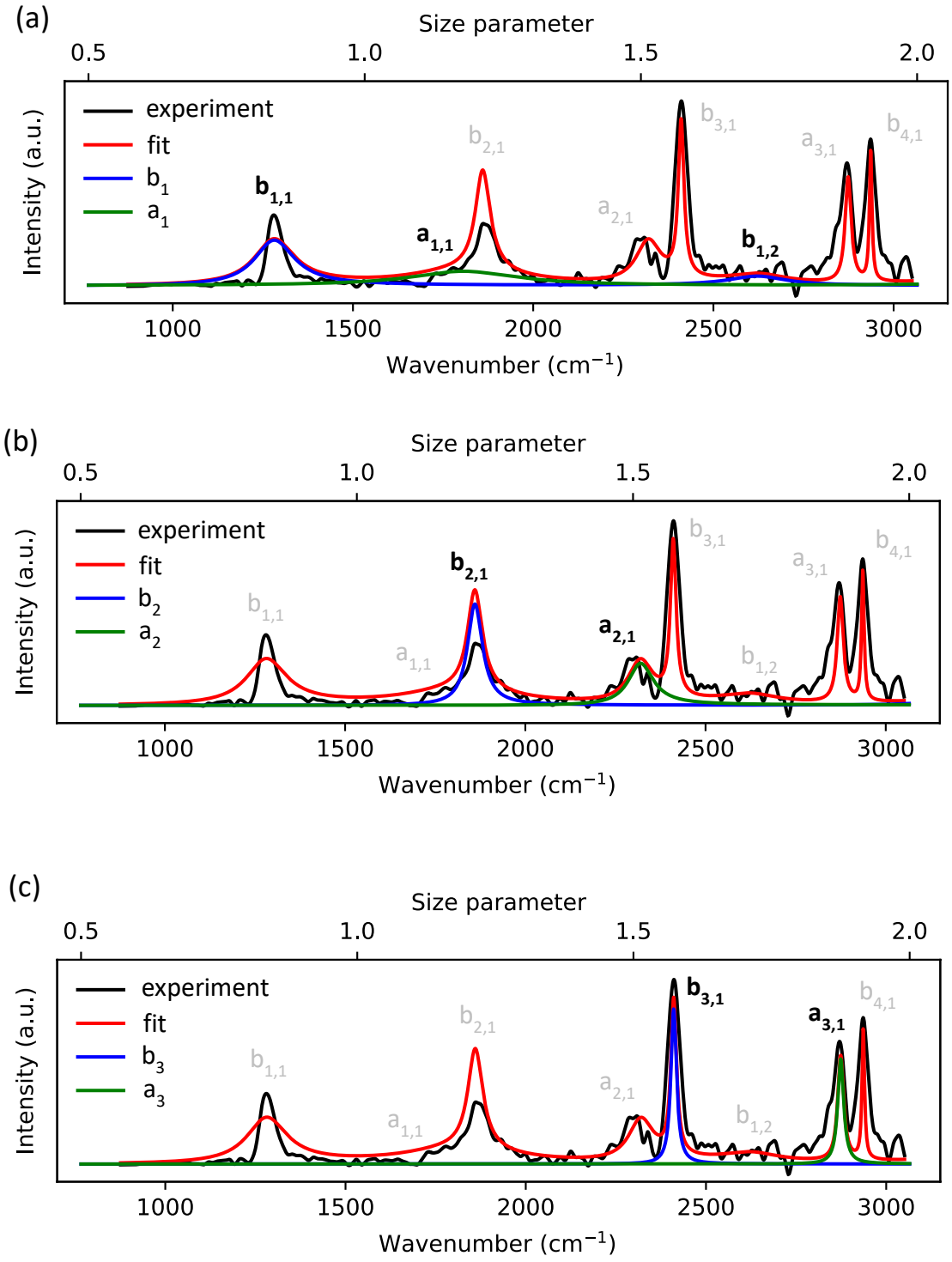
(a)
Size parameter
0.5
1.0
1.5
2.0
experiment
fit
b1
a1
Intensity (a.u.)
b1,1
a1,1
b2,1
a2,1
b3,1
b1,2
a3,1
b4,1
1000
1500
2000
2500
3000
Wavenumber (cm−1)
(b)
Size parameter
0.5
1.0
1.5
2.0
experiment
fit
b2
a2
Intensity (a.u.)
b1,1
a1,1
b2,1
a2,1
b3,1
b1,2
a3,1
b4,1
1000
1500
2000
2500
3000
Wavenumber (cm−1)
(c)
Size parameter
0.5
1.0
1.5
2.0
experiment
fit
b3
a3
Intensity (a.u.)
b1,1
a1,1
b2,1
a2,1
b3,1
b1,2
a3,1
b4,1
1000
1500
2000
2500
3000
Wavenumber (cm−1)

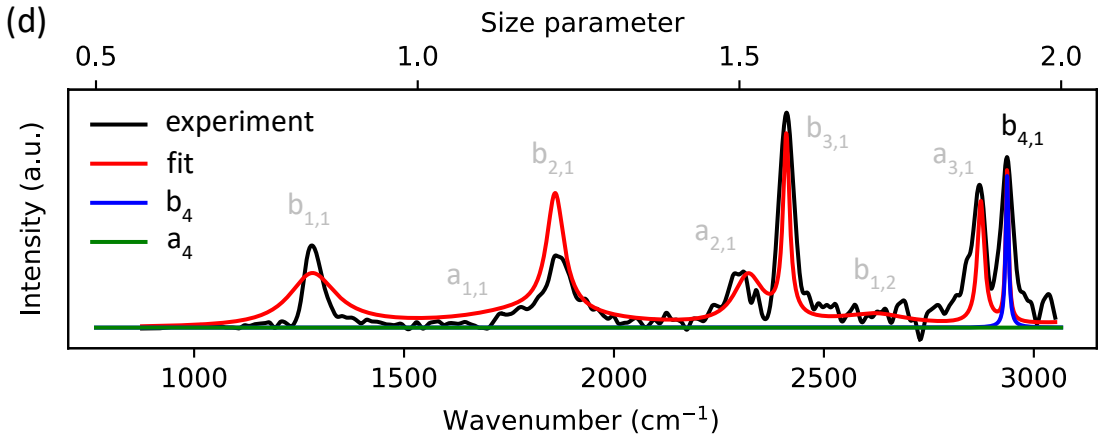

Figure S7. Experimental emission spectra for M1 (black curve), theoretical fitted spectra considering all the multipoles of the Mie series (red curve) and theoretical spectra considering single multipolar b_n (blue curve) and a_n (green curve) terms: (a) b_1 and a_1; (b) b_2 and a_2; (c) b_3 and a_3; (d) b_4 and a_4. The resonances associated with the corresponding multipolar terms are indicated in black letters while the other ones are indicated in grey letters.

S4. Thermal emission spectra of other silicon microspheres.

We show in this section the measured thermal emission spectra (black curves) of several silicon microspheres with different diameters (Φ) and fitted temperatures (T), and their theoretical fit to eq. (1) of the main text (red curves).

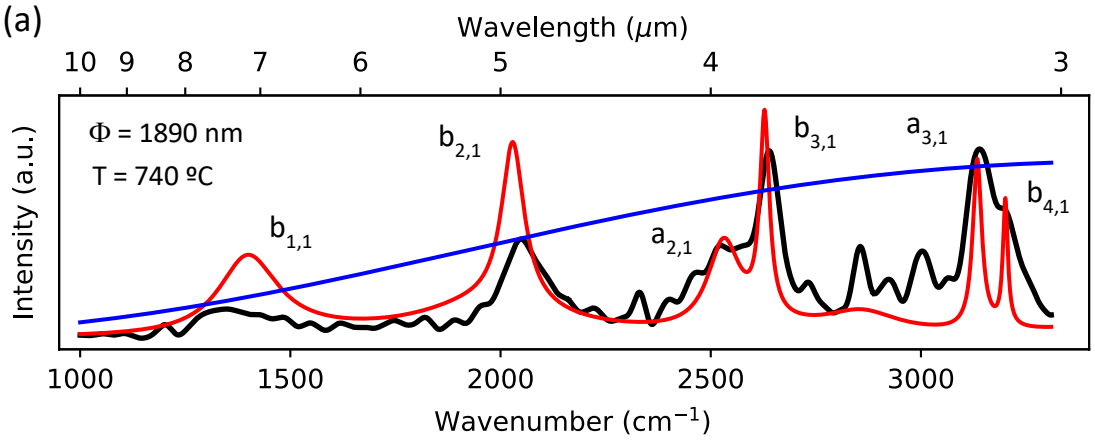

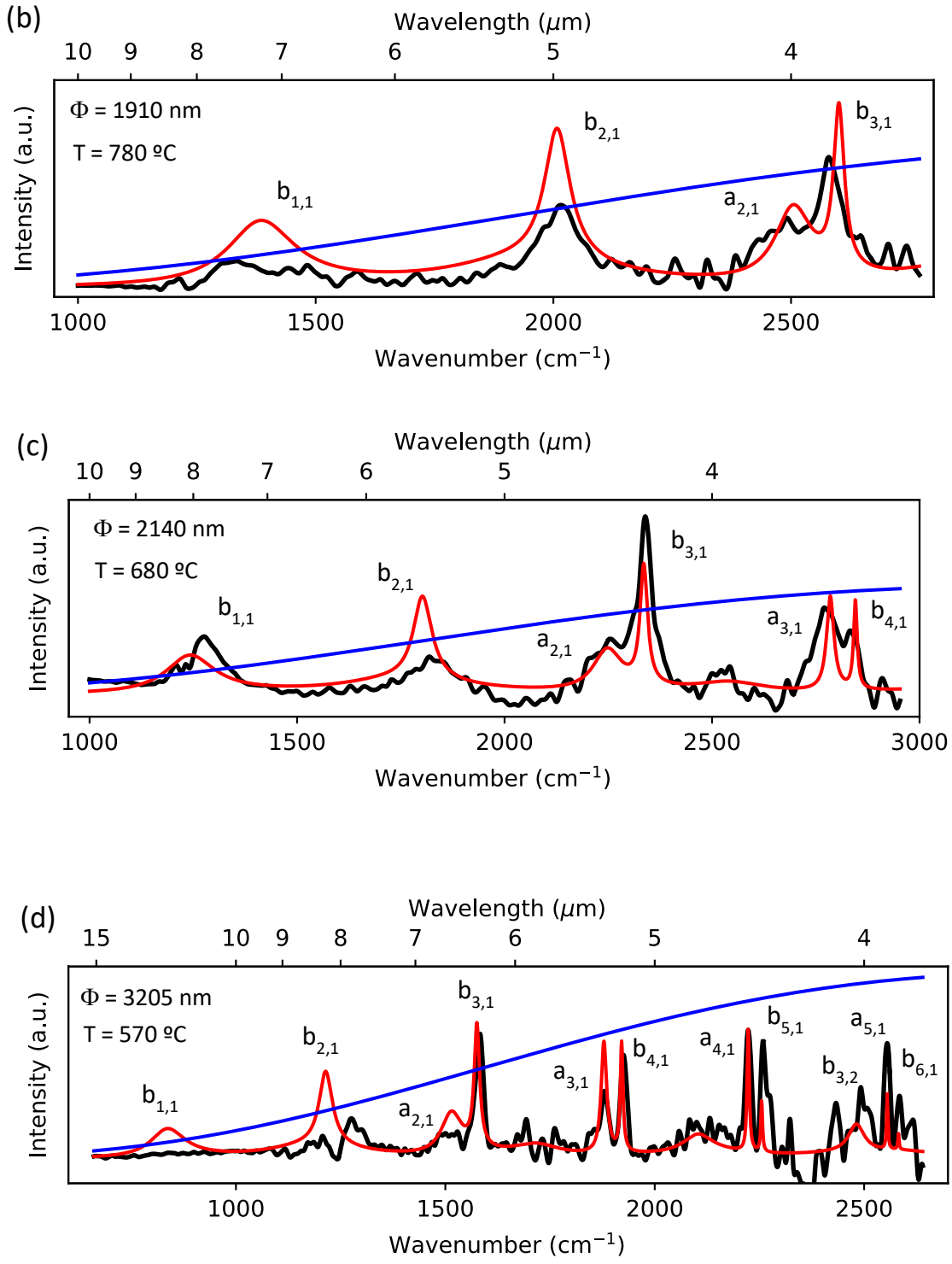
(b)
Wavelength (μm)
10 9 8 7 6 5 4
Φ = 1910 nm
T = 780 ºC
b1,1
b2,1
a2,1
b3,1
Intensity (a.u.)
1000 1500 2000 2500
Wavenumber (cm−1)
(c)
Wavelength (μm)
10 9 8 7 6 5 4
Φ = 2140 nm
T = 680 ºC
b1,1
b2,1
a2,1
b3,1
a3,1
b4,1
Intensity (a.u.)
1000 1500 2000 2500 3000
Wavenumber (cm−1)
(d)
Wavelength (μm)
15 10 9 8 7 6 5 4
Φ = 3205 nm
T = 570 ºC
b1,1
b2,1
a2,1
b3,1
a3,1
b4,1
a4,1
b5,1
b3,2
a5,1
b6,1
Intensity (a.u.)
1000 1500 2000 2500
Wavenumber (cm−1)

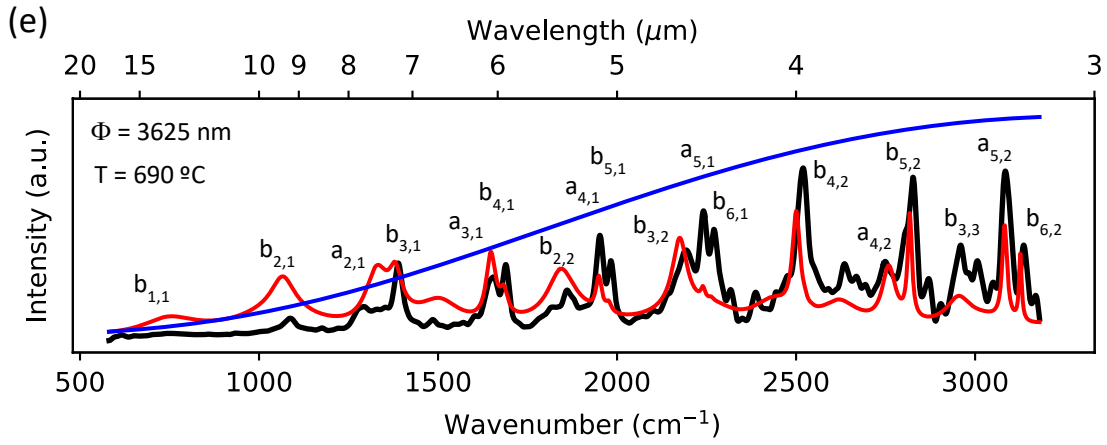

Figure S8: (a), (b), (c), (d) (e) Measured thermal emission spectra (black curves) of several silicon microspheres at different temperatures and their theoretical fit to eq. (1) of the main text (red curves). The sphere diameter (Φ) and the fitted temperature are indicated in each subplot. In addition, Mie resonances are identified and indicated beside their corresponding peak. The blue lines correspond to the calculated emission of a black body that has an area equal to the geometric projected area of the microsphere.

S5. Lorentizan fits to resonance peaks of M2.

The quality factor, Q, of a resonant peak can be calculated as $Q=\lambda_0/\Delta\lambda$ where λ_0 is the center of the peak and $\Delta\lambda$ is its full width at half maximum. In order to calculate the Q for peaks $a_{5,1}$ and $b_{6,1}$ of sample M2 (ϕ = 3730 nm, T = 560 ºC) plotted in figure 3 (b), that part of the spectrum including both peaks was assumed to follow a superposition curve of two lorentizan functions. The corresponding fitting process was performed for both the experimental (Figure S9) and the theoretical (Figure S10) spectra. The results of the fits are summarized in Table S1 and Table S2 respectively. Figure S9 shows, in addition, the decomposition of the two lorentzian functions.

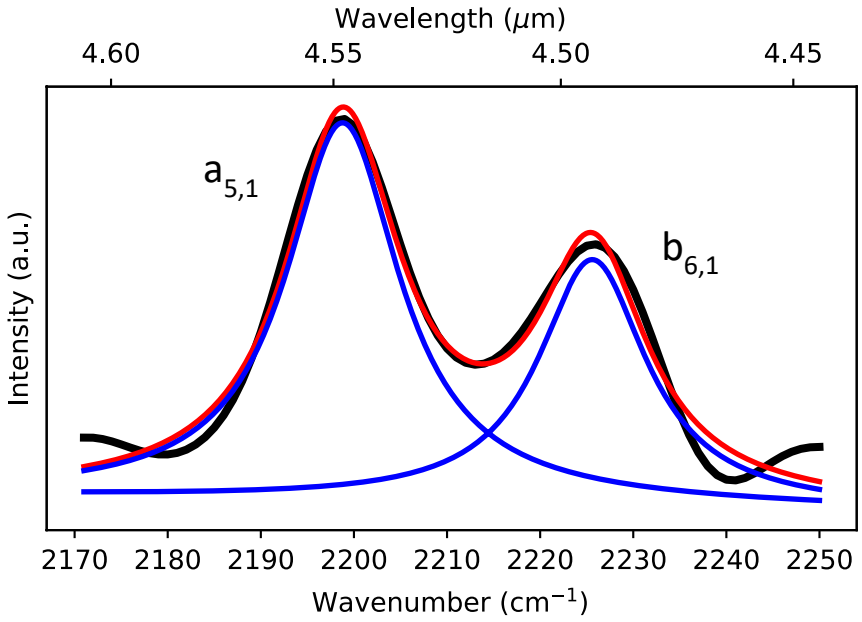

Figure S9. Experimental spectrum (black curve) of M2 (ϕ = 3730 nm, T = 560 ºC) at the spectral zone of modes $a_{5,1}$ and $b_{6,1}$. The red curve corresponds to the fit to the superposition of two lorentzian functions (see Table S1) that have been plotted in blue.

Table S1. Main fitting parameters of the experimental spectrum of Figure S9 to the superposition of two Lorentzian funcions centered at X_0 and with a HWHM (half width at half maximum) of Γ, and calculated quality factor, Q.

Mode	X_0 (cm^{-1})	Γ (cm^{-1})	Q $[X_0/(2\Gamma)]$
$a_{5,1}$	2198.79 ± 0. 06	7.4 ± 0. 1	149 ± 1
$b_{6,1}$	2225.61 ± 0. 09	7.0 ± 0. 2	159 ± 2

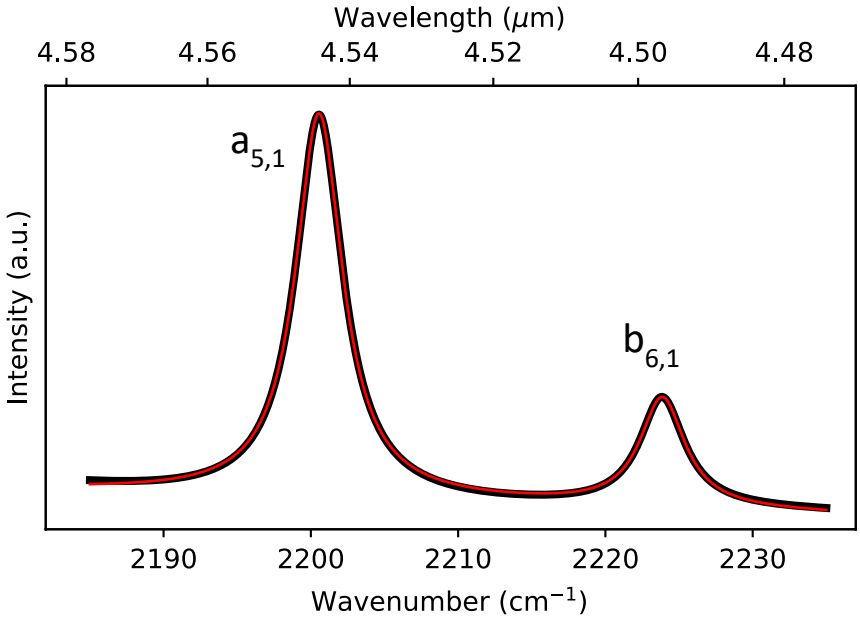

Figure S10. Theoretical spectrum (black curve) of M2 at the spectral zone of modes $a_{5,1}$ and $b_{6,1}$ corresponding to equation (1) of the Main text. The red curve corresponds to the fit to the superposition of two lorentzian curves (see Table S2).

Table S2. Main fitting parameters of the theoretical spectrum of Figure S10 to the superposition of two Lorentzian funcions centered at X_0 and with a HWHM of Γ, and calculated quality factor, Q.

Mode	X_0 (cm^{-1})	Γ (cm^{-1})	Q [$X_0/(2\Gamma)$]
$a_{5,1}$	2200.55 ± 0.01	1.93 ± 0.02	570 ± 3
$b_{6,1}$	2223.87 ± 0.04	1.85 ± 0.07	601 ± 11

References

[1] Peter R. Griffiths, James A. de Haseth, *Transform Infrared Spectrometry*, John Wiley & Sons, New Jersey, **2007**.

[2] T. Sato, Jpn. *J. Appl. Phys*. ***1967***, 6, 339.

[3] R. Fenollosa, F. Ramiro-Manzano, M. Garín, R. Alcubilla, *ACS Photonics* **2019**, 6, 3174.

[4] C. F. Bohren, D. R. Huffman, *Absorption and Scattering of Light by Small Particles*. John Wiley & Sons: New York, **1998**.

[5] R. Fenollosa, F. Meseguer, M. Tymczenko, *Adv. Mater*. **2008**, 20, 95.